Supplementary data to MS "Macrophage-mediated phagocytosis of apoptotic cholangiocytes contributes to reversal of biliary fibrosis" by Popov et al.

Supplementary table 1. Primers and probes used in quantitative RT-PCR (see M&M for details).

Target gene	5´-Primer	TaqMan probe	3´-Primer
β2MG	CCGATGTATATGCTTGCAGAGTTAA	AACCGTCACCTGGGACCGAGACATGTA	CAGATGATTCAGAGCTCCATAGA
procollagen α1(I)	TCCGGCTCCTGCTCCTCTTA	TTCTTGGCCATGCGTCAGGAGGG	GTATGCAGCTGACTTCAGGGATGT
procollagen α2(IV)	AGCTCCTGACCCCGAGGTTA	----	AGCCCCACTGTCACAGTCG
integrin β6	AACGATCAAAGCCAAGTGG	AAACGGGAACCAATCCGCTGTACCG	TCTTAAAAGTGCTGGTGGAGCCC
TIMP-1	TCCTCTTGTTGCTATCATTGATAGCTT	TTCTGCAACTCGGACCTGGTTATAAGG	CGCTGGTATAAGGTGGTCTCGAT
TIMP-2	GCTGGACGTTGGAGGAAAGA	TCTCCTTCCGCCTTCCCTGCAATTAGA	GCACAATAAAGTCACAGAGGGTAAT
TGFβ1	AGAAGTCACCCGCGTGCTAA	ACCGCAACAACGCAATCTATGACAAAACCA	TCCCGAATGTCTGACGTATTGA
TGFβ2	CCAAGAGCTGGAGGCGAG	TCGCAGGTATCGATGGCACCTCC	TTTCTGATCACCACTGGCATATG
MMP-2	CCGAGGACTATGACCGGGATAA	TCTGCCCCGAGACCGCTATGTCCA	CTTGTTGCCCAGGAAAGTGAAG
MMP-3	CCGTTTCCATCTCTCTCAAGATGA	AGATGGTATTCAATCCCTCTATGGACCTCC	CAGAGAGTTAGATTTGGTGGGTACCA
MMP-8	CCTAGTTTTCTTATTTAAAGGCAGACAGTA	GCTGCAAGTCATAGGCACTTAGAGCCCA	ACTCCTTGGGAATCCATAGTTGG
MMP-9	CATGAAGACGACATAAAAGGCATC	CAGGTTTAGAGCCACGACCATACAGATGCT	GGCTGGAGGCCTTGGG
MMP-12	GCAGTGCCCCAGAGGTCA	AGATCCTGTAAGTGAGGTACCGCTTCATCCA	CGCTCCAGACTTGAAAAGCTTT
MMP-13	GGAAGACCCTCTTCTTCTCA	TCTGGTTAGCATCATCATAACTCCACACGT	TCATAGACAGCATCTACTTTGTC
MMP-14	GAACTTTGACACCGTGGCCAT	CAGAACCATCGCTCCTTGAAGACAAACATC	CCGTCCATCACTTGGTTATTCCT
α-SMA	GCTGACAGGATGCAGAAGGA	CACCATGAAGATCAAGATTATTGCTCCTCCAG	GCCGATCCAGACAGAATATTTG
PDGFR-B	TGGTCCTTTGGAATCCTACTCTG	AAATCTTCACACTGGGTGGCACCCCTT	GGTCGTTCATGGGCAGCT
CTGF	ATCCCTGCGACCCACACAAG	CTCCCCCGCCAACCGCAAGAT	CAACTGCTTTGGAAGGACTCGC
PAI-1	GGCTCAGAACAACAAGTTCAACTACA	TGAGTTCACCACTCCGGATGGGC	CAGTTCCAGGATGTCGTACTCG
uPA	TGACCCAGAGTGGAAAACAGATT	GAGGTCCTCCTGAATCTCCCGAGCA	GGGCGGCCATCGATG
UPAR-1	CGGTGCATACAGTGCGAAAGT	----	AGGTGCAGGATGCACACTCAA

Supplementary Table 2. Dynamics of body and liver weight, and serum markers of inflammation and cholestasis during fibrosis induction and resolution. Parameters were determined at sacrifice in rats after 4 weeks of BDL (BDL4w, n=6), and 3, 7, 14 days, 4 and 12 weeks after RY-anastomosis (RY3d, n=4, RY7, 14d, 4w and 12w, n=6, respectively). Sham-operated rats (Sham, n=8) served as normal controls.

	Sham	BDL 4w	RY 3d	RY 7d	RY 14d	RY 4w	RY 12w
ALT, U/l	26.6±6.3	65.4±19.1*	21.1±6.5^{+}	33.0±4.1^{+}	35.1±14.7^{+}	41.8±7.4^{+}	44.5±8.2^{+}
AST, U/l	163±12	750±127*	191±21^{+}	207±21^{+}	219±31^{+}	177±31^{+}	256±34^{+}
ALP, U/l	156±36	371±62*	174±35^{+}	146±40^{+}	156±54^{+}	203±78^{+}	174±92^{+}
GGT, U/l	<2.5	57.2±19.0*	<5^{+}	<5^{+}	<5^{+}	<2.5^{+}	<2.5^{+}
Bilirubin, μM/l)	1.4±0.2	76.0±23.7*	9.6±2.4^{+}	4.5±1.5^{+}	1.9±0.7^{+}	2.0±0.4^{+}	2.3±0.8^{+}
Body weight, g	405 ± 17	394 ± 13	388 ± 13	402 ± 9	417 ± 8	429 ± 6	436 ± 8
Liver weight, g	13.4 ± 1.7	34.3 ± 5.0*	24.3 ± 2.2^{+}	20.3 ± 1.6^{+}	18.3 ± 3.4^{+}	15.7 ± 2.0^{+}	15.2 ± 2.4^{+}
Liver/body weight, %	3.30 ± 0.32	8.70 ± 0.98*	6.24 ± 0.38^{+}	5.06 ± 0.31^{+}	4.39 ± 0.75^{+}	3.64 ± 0.41^{+}	3.48 ± 0.5^{+}

* - $p<0.05$ compared to sham-operated group; $^{+}$ - $p<0.05$ compared to the peak fibrosis group (BDL4w).

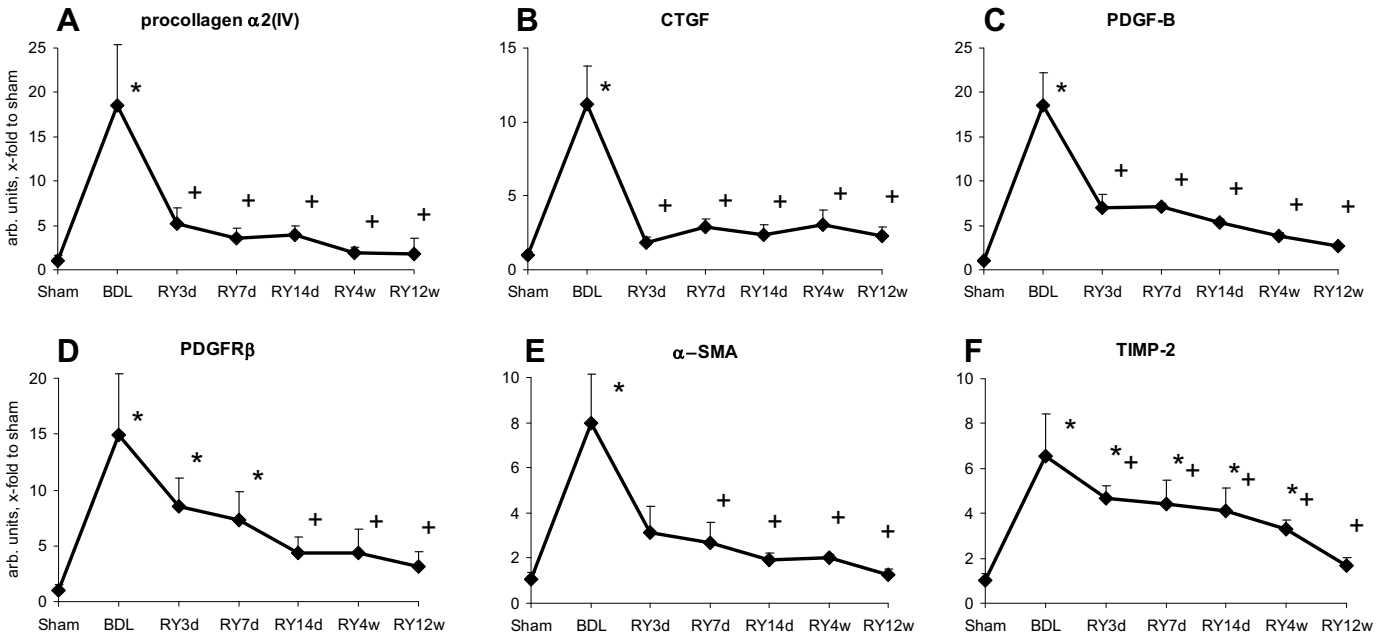

Supplementary figure 1. Two distinct profibrogenic transcript profiles during fibrosis progression and reversal. "Cholangiocyte-specific" transcripts: procollagen α2(IV) (A), connective tissue growth factor CTGF (B), platelet derived growth factor B PDGF-B (C) which are rapidly downregulated after RY-anastomosis; "HSC/MF-specific" transcripts: PDGF receptor beta (PDGFR-β) (D), α-SMA (E) and TIMP-2 (F) which show a delayed downregulation. Quantification by Real Time quantitative PCR (see also Fig.2 of main manuscript and references 33, 35, 32, 21, 36 in main manuscript for cellular sources of respective transcripts) was performed in total hepatic RNA. Data are expressed as means±SEM, and in arbitrary units relative to β2MG mRNA (fold change vs. sham-operated controls). *$p<0.05$ compared to the sham-operated group; $^{+}p<0.05$ compared to the peak of fibrosis group (BDL).

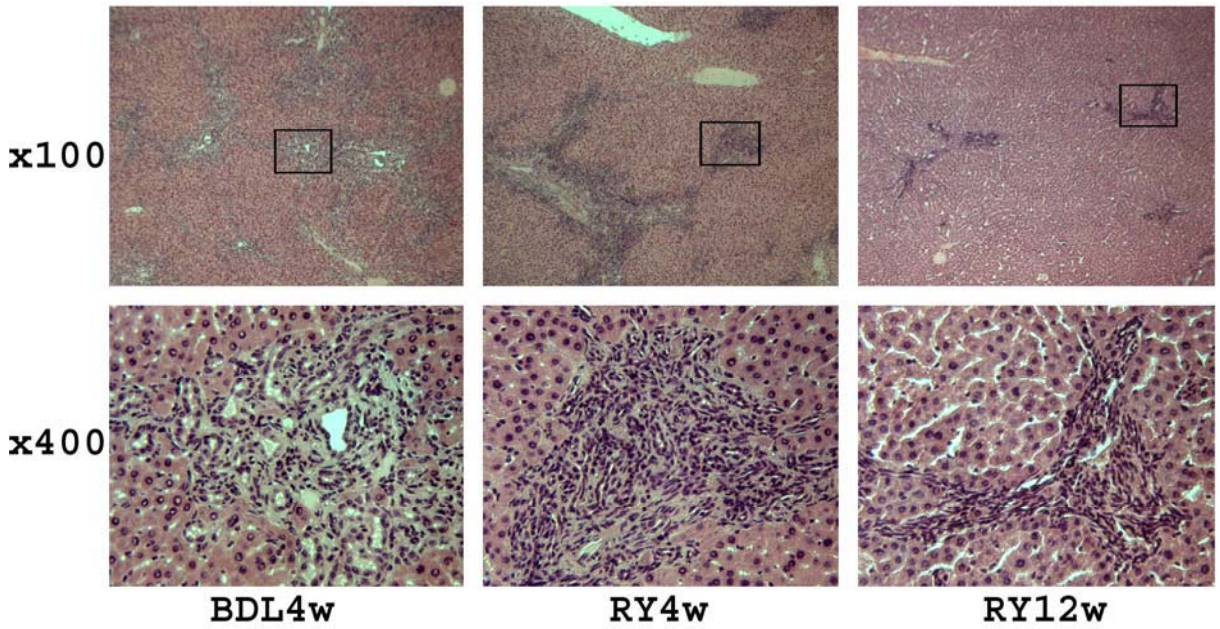

Supplementary figure 2. Portal and septal areas are densely populated with cells throughout reversal of biliary fibrosis. Reversal of BDL-induced fibrosis after RY-anastomosis. Portal and septal areas become "hypercellular" during reversal. Hypercellularity persists even in the remaining mildly enlarged portal tract at week 12 of reversal, indicating that remodeling of the scar is a cell-mediated process. While α-SMA is readily detected in activated HSC/MF around proliferating bile ducts at the peak of BDL-fibrosis, septal cells lose positivity of the HSC activation marker α-SMA immediately (at day 3) after RY-anastomosis (data not shown). Representative pictures, H&E staining.

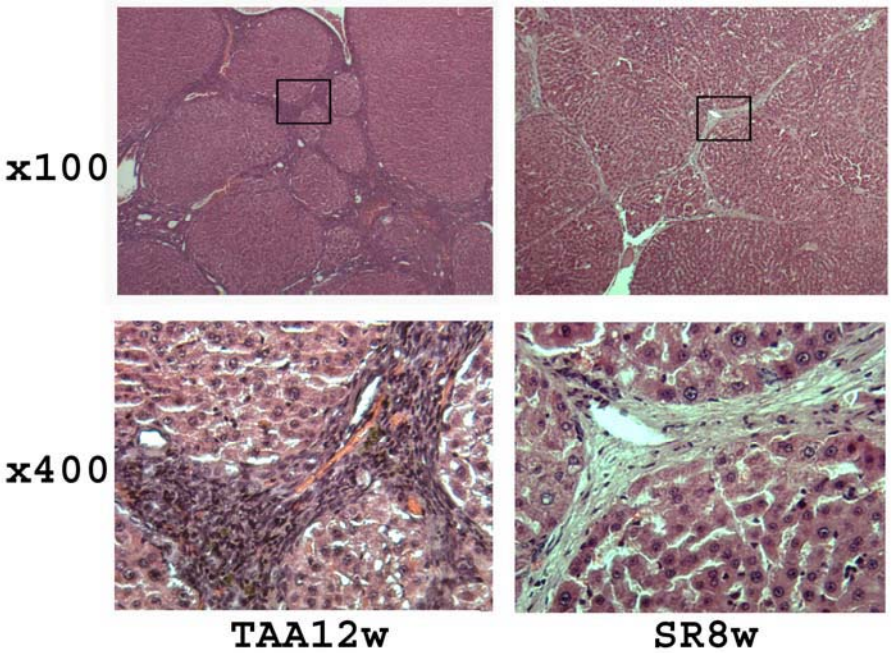

Supplementary figure 3. Septa become depopulated in "irreversible" liver fibrosis. Hepatotoxin-induced rat liver fibrosis was induced by intraperitoneal thioacetamide (TAA) injection (200mg/kg twice weekly for 12 weeks) and animals were allowed to recover for additional 8 weeks as described before(Popov et al. 2006 ref. 6, main manuscript). Septal areas are highly populated at peak of TAA-

fibrosis (TAA12w) but become "hypocellular" 8 weeks after TAA discontinuation (SR8w). There is no spontaneous reversal after 8w of TAA withdrawal (Popov et al, 2006, ref. 6, main manuscript). These findings are similar to findings reported in incomplete reversal of advanced CCl_4-induced fibrosis in rats (Issa et al, 2004, ref. 8, main manuscript). Representative pictures, H&E staining.

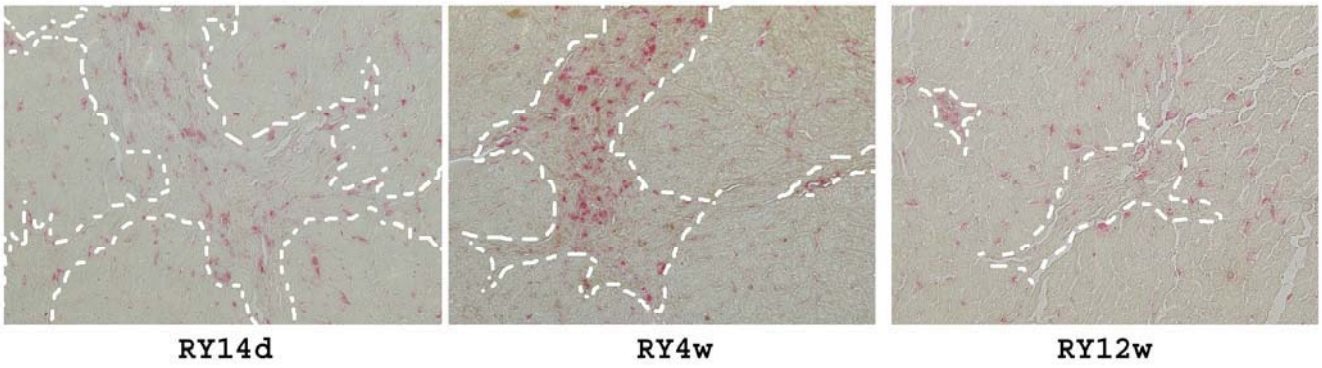

Supplementary figure 4. Increase in CD68+ cells in scarred portal tracts indicates active macrophage recruitment at the peak of reversal (RY4w). The connective tissue area in each representative picture is highlighted by a broken white line. Note that there is no change in the number and distribution of resident macrophages (Kupffer cells) in the parenchyma. Immunohistochemistry for CD68 (macrophage marker, red). Original magnification x20.

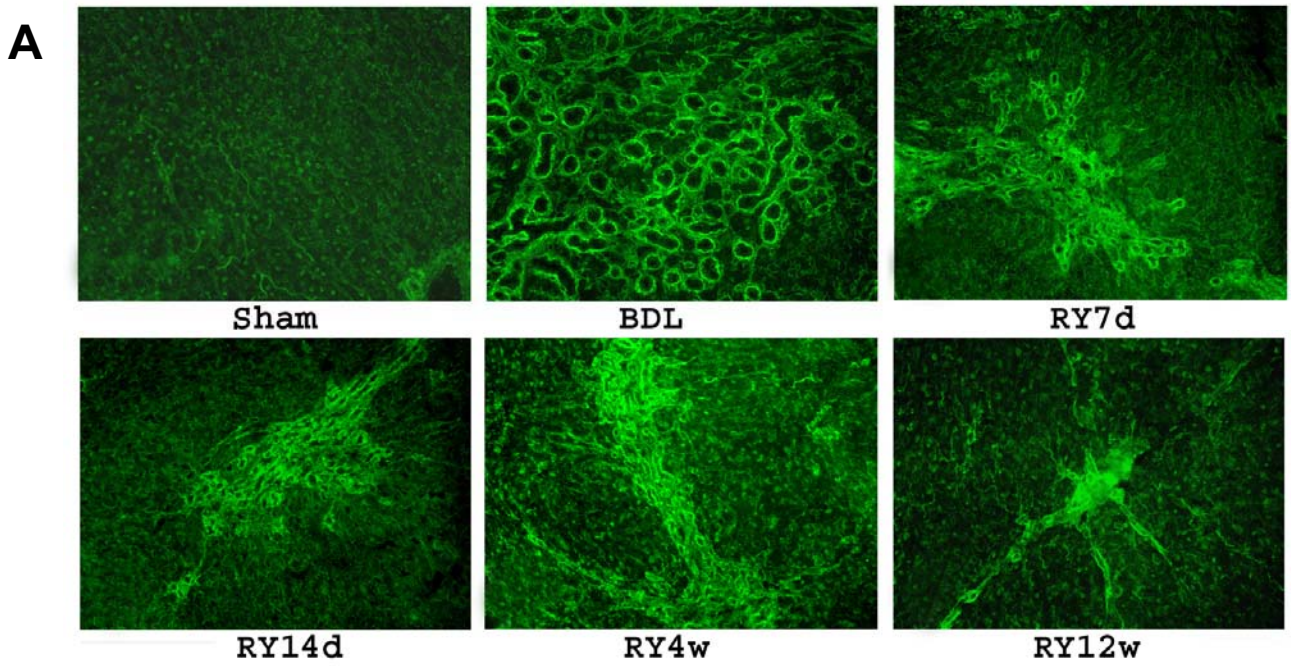

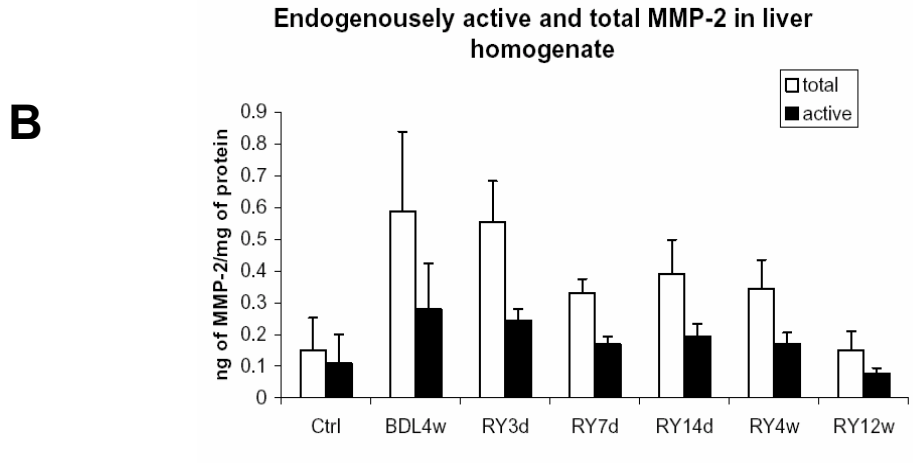

Supplementary figure 5. A: Mapping of gelatinase activity by in situ zymography reveals its association with the portal connective tissue at any time-point tested: representative images, magnification x200. **B: MMP-2 expression and activity declines during fibrosis reversal.** Total and active forms of MMP-2 in liver homogenates were determined by an ELISA-based activity assay (MMP-2 Biotrack Assay, Amersham, UK) after normalization to total protein content. See also Fig. 5A in the main manuscript for the corresponding MMP-2 zymography and Fig. 5B MMP-2 mRNA levels in total hepatic RNA.